Desalination and Water Treatment
www.deswater.com
doi: 10.1080/19443994.2014.937760

54 (2015) 1003–1012
April

Taylor & Francis
Taylor & Francis Group

Optimization of the UV/chlorine process for ammonia removal and disinfection by-products reduction

Xinran Zhang[a], Weiguang Li[a,b,*], Xujin Gong[a], Wenbiao Fan[a], Pengfei Ren[a]

[a]*School of Municipal and Environmental Engineering, Harbin Institute of Technology, Harbin 150090, P.R. China, Tel. +1 7654261576; email: zhangxinranhit@163.com (X. Zhang), Tel. +86 13904512510; emails: liweiguanghit@163.com, hitlwg@126.com (W. Li), Tel. +86 13936176182; email: kimkung@126.com (X. Gong), Tel. +86 13029992701; email: fwb666@126.com (W. Fan), Tel. +86 15114562108; email: pengfeiren84@163.com (P. Ren)*
[b]*State Key Laboratory of Urban Water Resource and Environment, Harbin Institute of Technology, Harbin 150090, P.R. China*

Received 6 January 2014; Accepted 16 June 2014

ABSTRACT

In this study, response surface methodology was used to investigate the efficiency of the UV/chlorine process for ammonia removal and disinfection by-products reduction. A five-level three-factorial central composite design was employed to study the interaction of three independent variables, including the Cl/N molar ratio, UV dose, and pH. Ammonia removal rate and trihalomethanes (THMs) formation rate were the target responses and two quadratic models were established. The optimum conditions of maximum ammonia removal and minimum THMs formation were: Cl/N molar ratio 0.99, UV dose 93.10 mJ cm^{-2}, and pH value 7.88, respectively. Under these conditions, the predicted ammonia removal rate and THMs formation rate by the two quadratic models were 64.03 and 34.87%, which were consistent with the verification experimental results.

Keywords: Central composite design; Ammonia; Disinfection by-products; UV/chlorine process

1. Introduction

In recent years, the pollution of ammonia nitrogen and natural organic matter (NOM) are increasingly serious in drinking water source [1]. Chlorination of ammonia increase chlorine-based disinfectants consumption, thereby weakening water treatment efficiency and promoting disinfection by-products (DBPs) production [2,3]. To solve this problem, an efficient and safe process for ammonia removal and DBPs reduction is required.

As an advanced oxidation process, the UV/chlorine process was investigated and evaluated in some researches [4,5]. This process has been applied on emerging contaminants [6] and NOM removal [7,8]. In the UV/chlorine process, UV irradiation at 254 nm could photo-decompose free chlorine and generate several active species, including OH radicals and Cl radicals, which could remove NOM [9,10]. A recent

*Corresponding author.

Presented at the 6th International Conference on the "Challenges in Environmental Science and Engineering" (CESE-2013), 29 October–2 November 2013, Daegu, Korea

study also reported that the application of the combined medium pressure UV lamp and chlorine can effectively remove trihalomethanes (THMs) during swimming pool water treatment [11]. Furthermore, in ammonia-containing water treatment, the UV photolysis of chloramine occurred and produced more radicals [12]. However, to our best knowledge, studies on the UV/chlorine process for these two contaminants removal are limited.

The aim of this work is to investigate the efficiency of the UV/chlorine process for ammonia removal and DBPs reduction, simultaneously. The optimum operational condition of the UV/chlorine process was determined using response surface methodology (RSM), which was a statistical experimental design method [13,14]. Specifically, central composite design (CCD), as a RSM, offers more advantages compared with the conventional one-factor-at-a-time approach, including improving experiments efficiency, evaluating variables interactions, and optimizing reaction conditions [15–17]. Therefore, the experiments were designed and conducted according to CCD to optimize the UV/chlorine process parameters.

2. Materials and methods

2.1. Materials and chemicals

A stainless steel tubular reactor (1.5 L, $L = 610$ mm, $d = 80$ mm) equipped with a low pressure Hg lamp (25 W, HNG, Germany) was used in the experiments. The UV irradiation at 254 nm was 0.2 mW cm^{-2} measured by a UV radiometer (Model IL1400, International Light, USA). The reactor was closed except for three small openings for adding agent, adding water samples, and taking samples, respectively.

The filtered water samples were collected from a drinking water treatment plant (the seventh WTP, Harbin, China) in December. The concentration of ammonia and TOC in the water samples were 0.76 mg L^{-1} as N and 3.54 mg L^{-1}, respectively. Sodium hypochlorite solution (CAS number 7681-52-9) was purchased from Sigma-Aldrich (USA) to prepare the chlorine stock solution (100 mg L^{-1}). The ultra-pure water was used in all experiments for aqueous solution prepared.

2.2. Experiments and analysis methods

According to experimental design, the chlorine stock solution was diluted to desired concentration. To keep pH stable, 0.02 M phosphate buffer solution was added into the samples, and water samples pH value was adjusted to target value by 1 M NaOH or 0.5 M H_2SO_4. Then, the water samples and active chlorine (sodium hypochlorite solution) were fed into the photo reactor by peristaltic pump (BT300-2 J, Langer Corp., USA), respectively.

The water samples were taken regularly for the further product analysis. The concentration of ammonia was measured using an ion specific electrode (95-12, Orion Co., USA). The concentration of active chlorine was determined by the DPD colorimetric method. Solution pH was detected with a pH meter (720 A, Thermo Orion Co., USA). The total concentration of THMs, including chloroform, dichlorobromomethane, dibromochloromethane, and bromoform, was used to represent the amount of DBPs formation. The measurement of THMs followed the procedures described in US EPA Method 524.2. All experiments were measured three times and averaged. The ammonia removal rate and THMs formation rate were calculated using Eqs. (1) and (2). C_0 and C_t were initial concentration and final concentration, respectively.

$$\text{Ammonia removal rate}\,(\%) = \frac{C_0 - C_t}{C_0} \times 100 \quad (1)$$

$$\text{THMs formation rate}\,(\%) = \frac{C_t - C_0}{C_0} \times 100 \quad (2)$$

2.3. RSM experimental design

A three-factor five-level CCD was carried out to optimize the UV/chlorine process operating conditions. Table 1 shows the ranges and levels of the three independent variables, including the Cl/N molar ratio (X_1), UV dose (X_2), and pH value (X_3).

In this experimental design, Design Expert 8.0 software was used to design experiments and build the mathematical models. The two responses, ammonia removal rate and THMs formation rate, were fitted by

Table 1
Experimental ranges of the independent variables

Independent variables	Factors X_i	Ranges and levels				
		−1.68	−1	0	1	1.68
Cl/N molar ratio	X_1	0	0.3	0.8	1.3	1.6
UV dose/(mJ cm^{-2})	X_2	0	29.0	72.0	115.0	144.0
pH value	X_3	6.5	7.0	7.5	8.0	8.5

the empirical quadratic model, expressed as Eq. (3). In this equation, Y represented the response variable; X_i was independent variable, β_0, β_i, β_{ij}, and β_{ii} were the intercept, linear, interaction, and quadratic coefficients, respectively.

$$Y = \beta_0 + \sum_{i=1}^{k} \beta_i X_i + \sum_{i=1}^{j-1} \sum_{i=1}^{k} \beta_{ij} \cdot X_i \cdot X_j + \sum_{i=1}^{k} \beta_{ii} X_i^2 \quad (3)$$

3. Results and discussion

3.1. CCD model

Twenty-two experiments were designed and carried out, including eight cube points, six axial points, and six replications at the center point, plus two additional points. Table 2 presents the CCD factorial matrix and the experimental data. Under the experimental conditions, ammonia removal rate and THMs formation rate ranged from 14.89 to 73.63% and from 8.33 to 49.74%, respectively.

Table 3 shows the analysis of variance (ANOVA) for the regression parameters. The p values were less than 0.01 for all of the parameters, which indicated that both independent and quadratic factors were highly significant and imposed single and multiple effects on the two responses. Therefore, a quadratic model should be applied to fit the central composite models. Eqs. (4) and (5) show the equations of actual factors for the two responses, where Y_1 and Y_2 represent ammonia removal rate and THMs formation rate; X_1, X_2, X_3 represent independent variables of Cl/N molar ratio, UV dose, and pH, respectively.

$$\begin{aligned} Y_1\,(\%) = &-839.26 + 42.19 \cdot X_1 + 0.02 \cdot X_2 + 244.46 \cdot X_3 \\ &+ 0.08 \cdot X_1 \cdot X_2 + 2.28 \cdot X_1 \cdot X_3 + 0.02 \cdot X_2 \cdot X_3 \\ &- 17.15X_1^2 - 0.01X_2^2 - 14.89X_3^2 \end{aligned} \quad (4)$$

$$\begin{aligned} Y_2\,(\%) = &-899.68 + 23.02 \cdot X_1 + 0.06 \cdot X_2 + 235.25 \cdot X_3 \\ &- 0.21 \cdot X_1 \cdot X_2 + 4.82 \cdot X_1 \cdot X_3 - 0.03 \cdot X_2 \cdot X_3 \\ &- 15.28X_1^2 - 0.01X_2^2 - 15.50X_3^2 \end{aligned} \quad (5)$$

Table 2
Three factors CCD matrix and the value of response

	Real variables X_i			Responses Y_1		Responses Y_2	
	Cl/N molar ratio	UV dose (mJ cm^{-2})	pH	Ammonia removal rate (%)		THMs formation rate (%)	
Run	X_1	X_2	X_3	Observed	Predicted	Observed	Predicted
1	0.3	29.0	6.9	21.51	22.11	10.80	10.27
2	1.3	29.0	6.9	54.44	53.32	32.96	34.71
3	0.3	115.0	6.9	26.90	28.13	13.21	14.76
4	1.3	115.0	6.9	65.87	65.70	22.01	22.04
5	0.3	29.0	8.1	24.88	25.03	14.08	14.37
6	1.3	29.0	8.1	59.67	58.83	42.98	44.25
7	0.3	115.0	8.1	31.35	32.86	14.52	15.60
8	1.3	115.0	8.1	73.63	73.01	27.47	28.33
9	0.0	72.0	7.5	14.89	14.20	10.00	9.95
10	1.6	72.0	7.5	73.48	74.20	41.61	41.20
11	0.8	0.0	7.5	43.61	43.41	30.34	30.61
12	0.8	144.0	7.5	60.17	60.40	21.72	20.99
13	0.8	72.0	6.5	36.23	35.99	16.41	15.50
14	0.8	72.0	8.5	44.61	44.59	25.54	24.22
15	0.8	72.0	7.5	55.20	55.17	35.80	35.35
16	0.8	72.0	7.5	54.68	55.17	35.63	35.35
17	0.8	72.0	7.5	56.18	55.17	36.35	35.35
18	0.8	72.0	7.5	54.94	55.17	35.67	35.35
19	0.8	72.0	7.5	55.71	55.17	34.16	35.35
20	1.6	0.0	7.5	56.94	57.95	49.74	48.58
21	0.0	144.0	7.5	16.22	14.93	8.33	7.72
22	0.8	72.0	7.5	54.57	55.17	35.90	35.35

Table 3
ANOVA of the regression parameters

Regression	df	Sum of squares	Mean square	*F* value	*p*-value
Y_1 (ammonia removal rate, %)					
Linear	3.0	5,709.4	1,903.1	40.2	<0.0001
Quadratic	3.0	598.3	199.4	193.6	<0.0001
Y_2 (THMs formation rate, %)					
Linear	3.0	2,217.5	739.2	15.3	<0.0001
Quadratic	3.0	730.1	243.4	167.1	<0.0001

3.2. Model validation and statistical analysis

A "significant and adequate" model is essential to optimize the response surface [18,19]. The statistical testing of the two quadratic models was performed with *F*-test for ANOVA, as described in Table 4. The high R^2 values (0.998 and 0.994) indicated that 99.8 and 99.4% variations for ammonia removal and THMs formation were caused by the independent variables. Also, the *p* value of both responses was less than 0.001, which ensured that models were significant. In addition, the lack-of-fit estimates the variations around the fitted model relative to the pure error [20]. In this study, the lack-of-fit of the two models were not significant ($p = 0.08 > 0.05$), implying the two models were statistically significant.

Figs. 1(a) and 1(b) illustrate the relationship between the predicted values and actual values of the two responses. The predicted responses were calculated from the predicted models. As shown in Figs. 1(a) and 1(b), the observed values highly agreed with predicted responses, which indicated that the two quadratic regression models fitted well and could be used for prediction successfully.

3.3. Ammonia removal

Figs. 2(a)–(c) present the interactional effects of the three independent variables on ammonia removal. It indicated that the three factors affected ammonia removal significantly in the UV/chlorine process.

Fig. 2(a) shows the variation of ammonia removals with the change of Cl/N molar ratio and UV dose, while the pH value kept at central level. It is obvious that Cl/N molar ratio had significantly quadratic effects on ammonia removal. At low level of the Cl/N molar ratio (less than 0.8), the effects of UV dose on ammonia removal were slight. However, UV dose produced positive effects on ammonia removal when the Cl/N molar ratio kept at central or high level (0.8–1.6). When the Cl/N molar ratio fixed at 1, ammonia removals increased from 56 to 67% with the increase of UV dose from 30 to 115 mJ cm^{-2}. At high level of Cl/N molar ratio, monochloramine was the main compound in the solution which could photodecay by UV_{254} irradiation [10]. Therefore, UV irradiation at 254 nm and chlorine had synergistic effects on ammonia removal during the UV/chlorine process.

Table 4
ANOVA results of the two quadratic response surface models

Source	Sum of squares	df	Mean square	*F* value	*p*-value
Y_1 (ammonia removal rate, %)					
Model	6,548.40	9	727.60	706.39	<0.0001
Residual	12.36	12	1.03		
Lack of fit	10.41	7	1.49	3.80	0.08
Pure error	1.95	5	0.39		
Cor total	6,560.76	21			
$R^2 = 0.998$, Adj $R^2 = 0.997$, Pre $R^2 = 0.992$					
Y_2 (THMs formation rate, %)					
Model	3,040.46	9	337.83	231.92	<0.0001
Residual	17.48	12	1.46		
Lack of fit	14.71	7	2.10	3.79	0.08
Pure error	2.77	5	0.55		
Cor total	3,057.94	21			
$R^2 = 0.994$, Adj $R^2 = 0.990$, Pre $R^2 = 0.975$					

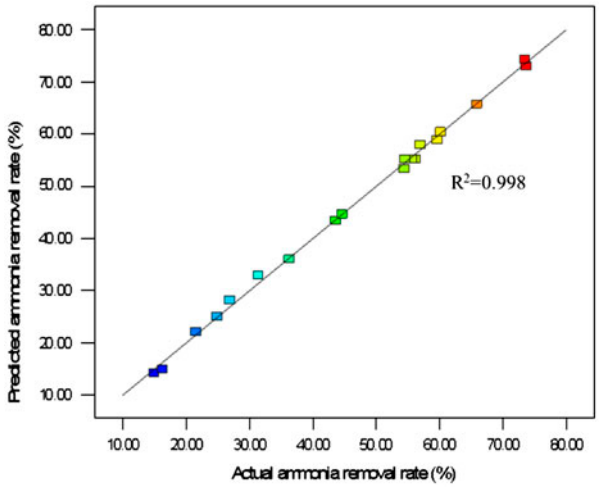

Fig. 1(a). Comparison between experimental results and predicted values by proposed model. Actual values vs. predicted values for ammonia removal.

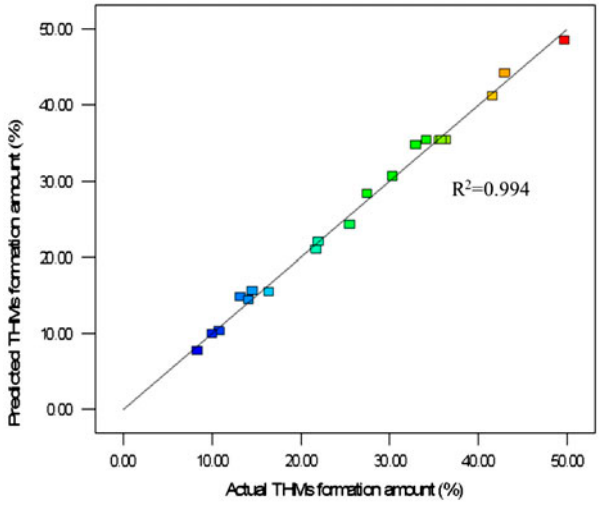

Fig. 1(b). Comparison between experimental results and predicted values by proposed model. Actual values vs. predicted values for THMs formation.

As shown in Fig. 2(b), when the UV dose was at central level (72 mJ cm^{-2}) and the Cl/N molar ratio fixed to 0.8, ammonia removal rate gradually increased from 47 to 55% with increasing pH from 7.0 to 7.5 and then decreased to 51% when pH at 8.0. The adverse effects with pH over than 7.5 were due to the fact that OCl^- was the dominant component in alkaline conditions. Furthermore, Fig. 2(c) also indicates pH value not always provide positive effect on ammonia removal. At the central condition of Cl/N molar ratio, the maximum ammonia removal obtained at the condition of UV dose 115 mJ cm^{-2} and pH 7.5.

As described in Eqs. (6)–(8), chlorine reacted with ammonia to form chloramine (mono-, di-, tri-) at low Cl/N molar ratio (<1.0) and oxidized into nitrogen gas at high Cl/N molar ratio (1.0–1.7), as described in Eq. (9) [21]. Thus, ammonia removal was obtained only when the Cl/N molar ratio was higher than 1.0. In addition, UV_{254} irradiation cannot photo decompose ammonia directly, which is consistent with the data in Table 2.

$$NH_3 + HOCl \leftrightarrow NH_2Cl + H_2O \quad (6)$$

$$NH_2Cl + HOCl \leftrightarrow NHCl_2 + H_2O \quad (7)$$

$$NHCl_2 + HOCl \leftrightarrow NCl_3 + H_2O \quad (8)$$

$$NH_4^+ + 1.5HOCl \leftrightarrow 0.5N_2 + 1.5H_2O + 2.5H^+ + 1.5Cl^- \quad (9)$$

In the UV/chlorine process, the ammonia removal efficiency was higher than either single chlorination or single UV_{254} irradiation at the same factorial values. Two possible pathways for ammonia removal in the UV/chlorine process: one is direct oxidation of ammonia by breakpoint chlorination process as mentioned above; the other is indirect photo decomposition of ammonia. The free chlorine and chloramine were photolytic by UV_{254} irradiation to form a series of powerful and non-selective radicals as the intermediates and generate nitrite, nitrate, and nitrous oxide as end-products, depicted as Eqs. (10)–(14) [12]. Because the Cl/N molar ratio was less than the molar ratio needed in breakpoint chlorination (1.7), the dominant pathway for ammonia removal followed the indirect oxidation method.

$$HOCl \xrightarrow{h\nu} \cdot OH + \cdot Cl \quad (10)$$

$$NH_3 + \cdot OH \rightarrow \cdot NH_2 + H_2O \quad (11)$$

$$NH_3 + \cdot Cl \rightarrow \cdot NH_2 + H^+ + Cl^- \quad (12)$$

$$\cdot NH_2 + \cdot OH \rightarrow NH_2OH \quad (13)$$

$$NH_2OH + \cdot OH \rightarrow NO_2^- \rightarrow NO_3^- \quad (14)$$

3.4. THMs formation

Figs. 3(a)–(c) illustrates the predicted 2D contour plots and 3D response surface plots which were drawn to investigate the interaction terms of three factors on THMs formation during the UV/chlorine process.

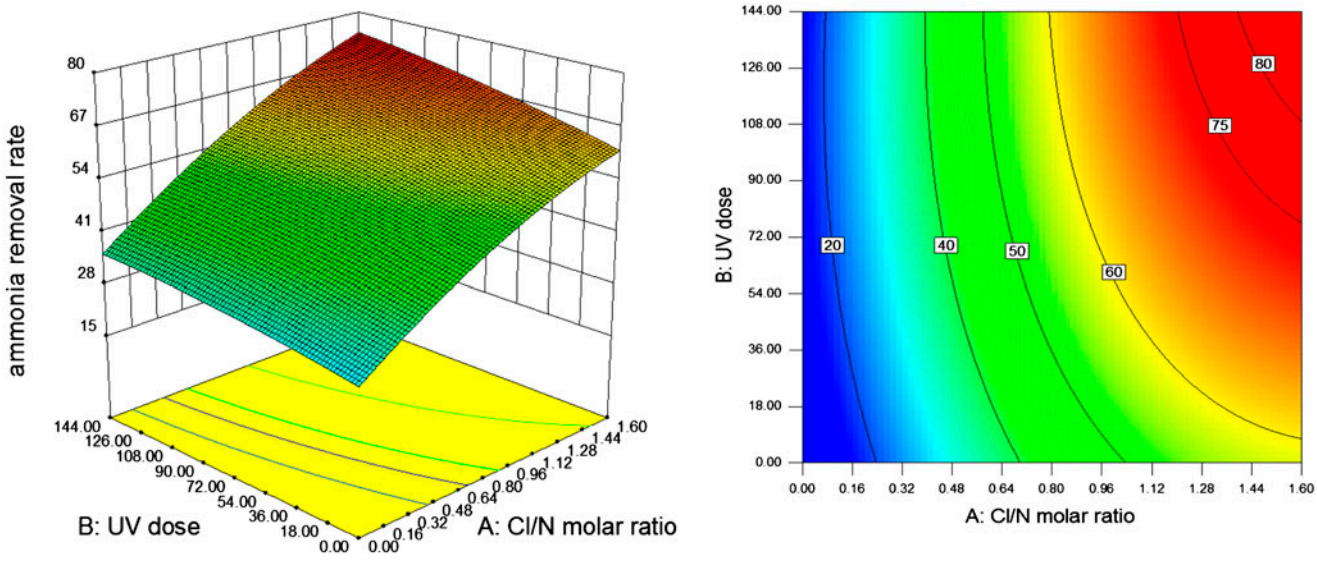

Fig. 2(a). Response surface (3D) and contour (2D) map for ammonia removal between independent variables. The interactional effects of Cl/N ratio and UV dose for ammonia removal.

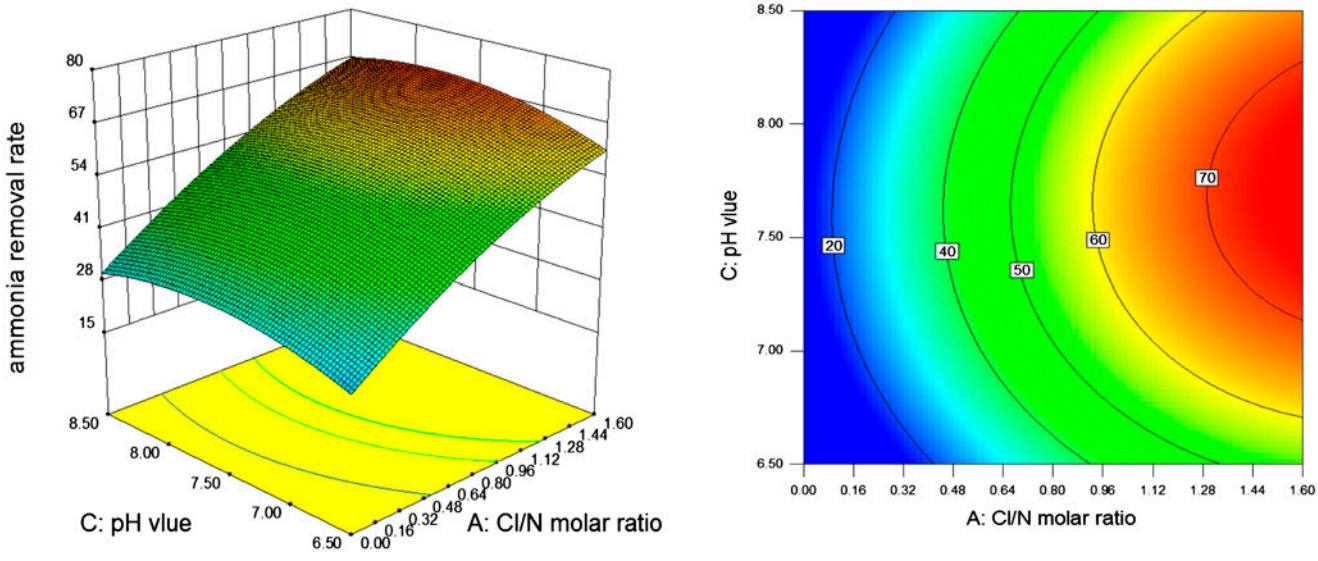

Fig. 2(b). Response surface (3D) and contour (2D) map for ammonia removal between independent variables. The interactional effects of Cl/N ratio and pH for ammonia removal.

Fig. 3(a) shows the THMs production decreased with the reduction of Cl/N molar ratio and the increase of UV dose, while the pH kept at central level. The increase of Cl/N molar ratio improved the THMs formation due to the fact that chlorination of natural organic compounds was the primary path for THMs generation. However, in the UV/chlorine process, chlorine and chloramine were photodecayed by UV_{254} irradiation. The products, such as OH radicals and Cl radicals could remove the THMs precursors and THMs simultaneously [8].

Fig. 3(b) illustrates that the THMs formation varied with the Cl/N molar ratio and pH value when the UV dose was at central level. The high level of Cl/N molar ratio provided more chlorine to react with THMs precursor, thereby increasing the THMs

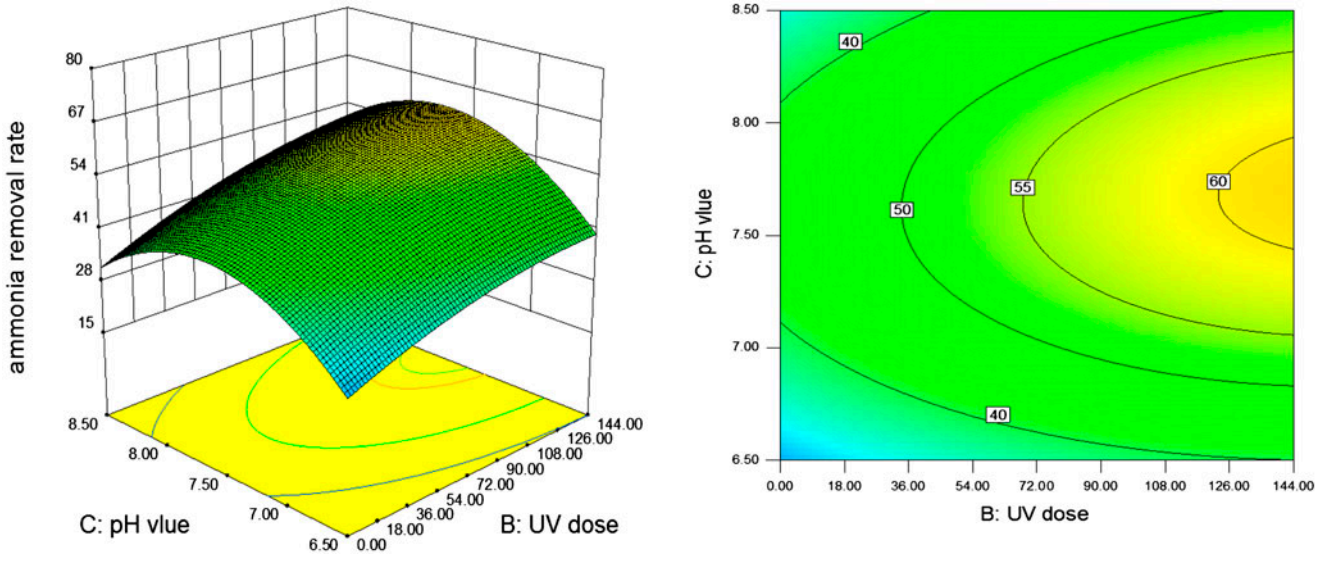

Fig. 2(c). Response surface (3D) and contour (2D) map for ammonia removal between independent variables. The interactional effects of UV dose and pH for ammonia removal.

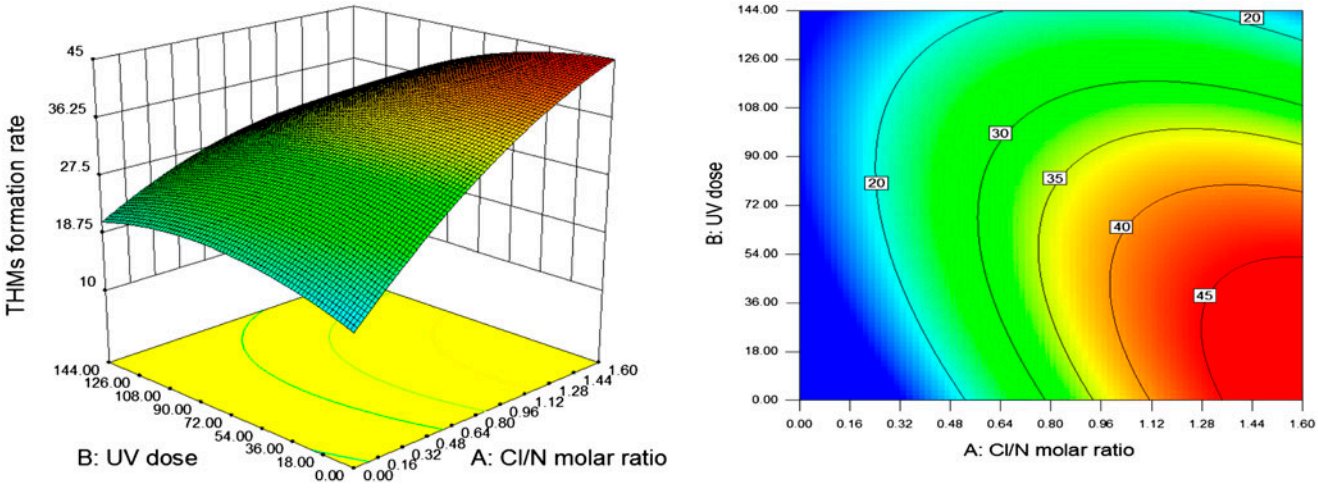

Fig. 3(a). Response surface (3D) and contour (2D) map for THMs formation between independent variables. The interactional effects of Cl/N ratio and UV dose for THMs formation.

formation. Furthermore, the pH value had a positive influence on THMs formation when the Cl/N molar ratio was fixed. This result indicated THMs were easier to generate in alkaline solution, which was in agreement with the former research [22]. In acid solution, HClO molecule was the dominant component which was more inclined to photo decomposition by UV_{254} irradiation than ClO^-. Therefore, the formation of THMs was restrained when pH was at the low level [23].

Fig. 3(c) provides more evidence that pH value and UV dose had an interactive influence on THMs formation. THMs formation decreased with the increase of UV dose and the decrease of pH value. In the UV/chlorine process, increasing the UV dose promoted the production of radicals, leading to the decrease of THMs formation. The low pH value was helpful to reduce the THMs formation, as mentioned above. In addition, THMs formation slightly decreased at a high level of pH value (around 8.0), because that

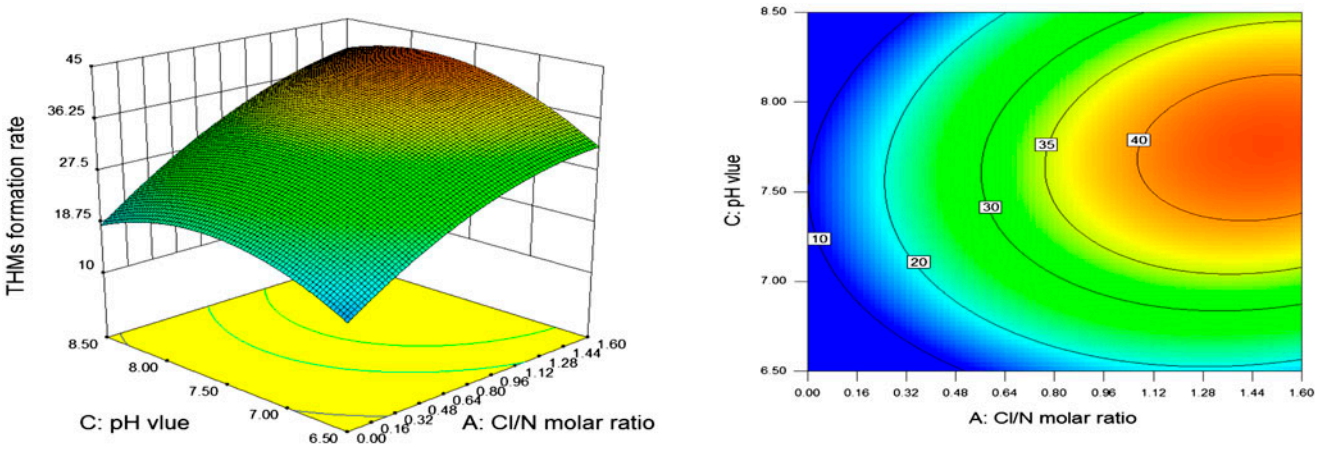

Fig. 3(b). Response surface (3D) and contour (2D) map for THMs formation between independent variables. The interactional effects of Cl/N ratio and pH for THMs formation.

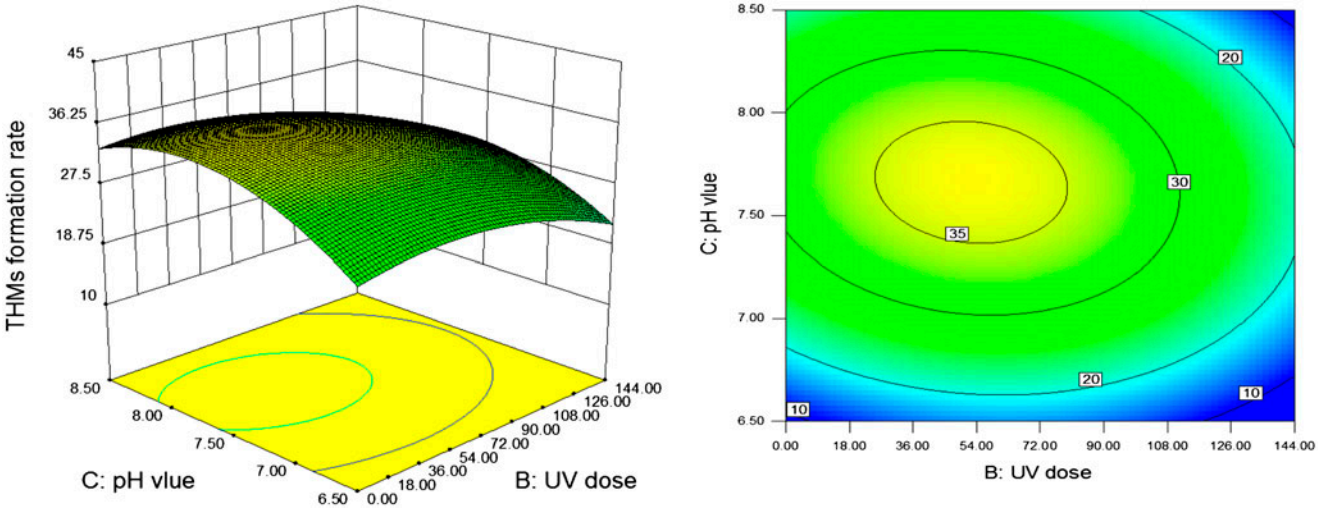

Fig. 3(c). Response surface (3D) and contour (2D) map for THMs formation between independent variables. The interactional effects of UV dose and pH for THMs formation.

alkaline solution could improve the oxidation property of the UV/chlorine process [24].

3.5. Optimization and model confirmation

A good optimization for practical application should consider the possibility of operation, economy, and maximization of results. In this study, efforts have been made to minimize both the Cl/N molar ratio and UV dose, as well as keep pH value in range of 6.5–8.5. The desired goal of this work was to maximize the ammonia removal and minimize THMs formation simultaneously.

According to the design models and the constraints as described, the optimal operating conditions of the UV/chlorine process were determined by ridge analysis using Design Expert 8.0.6.1 software. The optimum values for the maximum ammonia removal and the minimum THMs formation were Cl/N molar ratio 0.99, UV dose 93.10 mJ cm^{-2}, and pH value 7.88. Under these conditions, the predicted ammonia removal rate and THMs formation rate were 64.03 and 34.87%, respectively. It should be mentioned that, compared with chlorination, less chlorine dosage needed for ammonia removal and less THMs formation in the UV/chlorine process.

Furthermore, to verify these two models, confirmation tests were conducted under the optimum conditions. The experimental results were found to be 65.35% for ammonia removal and 33.47% for THMs formation, which closely agreed with the predicted values. The results demonstrated that the two models could successfully optimize the UV/chlorine process for ammonia removal and THMs formation.

4. Conclusions

This study investigated the efficiency of the UV/chlorine process for ammonia removal and THMs reduction. The three independent parameters (the Cl/N molar ratio, UV dose, and pH value) significantly influenced on the two responses, ammonia removal rate and THMs formation rate. Two quadratic models were established and fitted well to the experimental results, with high R^2 values (0.998 and 0.994). Under the restrains of minimal both the Cl/N molar ratio and UV dose and near to the natural pH, the optimization conditions for the maximum ammonia removal and minimum THMs formation were the Cl/N molar ratio 0.99, UV dose 93.10 mJ cm^{-2}, and pH 7.88, respectively. At the optimization condition, the predicted values of ammonia removal rate and THMs formation rate were 64.03 and 34.87%, respectively. These results were consistent with the corresponding experimental results.

Acknowledgment

This study was supported by the Heilongjiang Province Funds for Distinguished Young Scientists (JC200708).

References

[1] P. Kulkarni, S. Chellam, Disinfection by-product formation following chlorination of drinking water: Artificial neural network models and changes in speciation with treatment, Sci. Total Environ. 408 (2010) 4202–4210.
[2] H. Zhang, H.J. Liu, X. Zhao, J.H. Qu, M.H. Fan, Formation of disinfection by-products in the chlorination of ammonia-containing effluents: Significance of Cl_2/N ratios and the DOM fractions, J. Hazard. Mater. 190 (2011) 645–651.
[3] A.D. Shah, W.A. Mitch, Halonitroalkanes, halonitriles, haloamides, and N-nitrosamines: A critical review of nitrogenous disinfection byproduct formation pathways, Environ. Sci. Technol. 46 (2011) 119–131.
[4] J. Jin, M.G. El-Din, J.R. Bolton, Assessment of the UV/chlorine process as an advanced oxidation process, Water Res. 45 (2011) 1890–1896.
[5] P.Y. Chan, M.G. Gamal El-Din, J.R. Bolton, A solar-driven UV/Chlorine advanced oxidation process, Water Res. 46 (2012) 5672–5682.
[6] C. Sichel, C. Garcia, K. Andre, Feasibility studies: UV/chlorine advanced oxidation treatment for the removal of emerging contaminants, Water Res. 45 (2011) 6371–6380.
[7] X.R. Zhang, W.G. Li, P.F. Ren, Natural organic matter removal by UV/chlorine process: Modeling and optimization, Adv. Mat. Res. 807 (2013) 466–471.
[8] W. Liu, Z. Zhang, X. Yang, Y. Xu, Y. Liang, Effects of UV irradiation and UV/chlorine co-exposure on natural organic matter in water, Sci. Total Environ. 414 (2012) 576–584.
[9] M.J. Watts, K.G. Linden, Chlorine photolysis and subsequent OH radical production during UV treatment of chlorinated water, Water Res. 41 (2007) 2871–2878.
[10] L.H. Nowell, J. Hoigné, Photolysis of aqueous chlorine at sunlight and ultraviolet wavelengths—II. Hydroxyl radical production, Water Res. 26 (1992) 599–605.
[11] K. Hansen, R. Zortea, A. Piketty, S.R. Vega, H.R. Andersen, Photolytic removal of DBPs by medium pressure UV in swimming pool water, Sci. Total Environ. 443 (2013) 850–856.
[12] J. Li, E.R. Blatchley III, UV photodegradation of inorganic chloramines, Environ. Sci. Technol. 43 (2008) 60–65.
[13] C. Sahoo, A. Gupta, Optimization of photocatalytic degradation of methyl blue using silver ion doped titanium dioxide by combination of experimental design and response surface approach, J. Hazard. Mater. 215–216 (2012) 302–310.
[14] P.D. Saha, A. Dey, P. Marik, Batch removal of chromium(VI) from aqueous solutions using wheat shell as adsorbent: Process optimization using response surface methodology, Desalin. Water Treat. 39 (2012) 95–102.
[15] S. Chowdhury, P.D. Saha, Scale-up of a dye adsorption process using chemically modified rice husk: Optimization using response surface methodology, Desalin. Water Treat. 37 (2012) 331–336.
[16] E.E. Mitsika, C. Christophoridis, K. Fytianos, Fenton and Fenton-like oxidation of pesticide acetamiprid in water samples: Kinetic study of the degradation and optimization using response surface methodology, Chemosphere 93 (2013) 1818–1825.
[17] M. Kasiri, A. Khataee, Removal of organic dyes by UV/H_2O_2 process: Modelling and optimization, Environ. Technol. 33 (2012) 1417–1425.
[18] A. Khataee, B. Habibi, Photochemical oxidative decolorization of C. I. basic red 46 by UV/H_2O_2 process: Optimization using response surface methodology and kinetic modeling, Desalin. Water Treat. 16 (2010) 243–253.
[19] A. Alberti, A.A.F. Zielinski, D.M. Zardo, I.M. Demiate, A. Nogueira, L.I. Mafra, Optimisation of the extraction of phenolic compounds from apples using response surface methodology, Food Chem. 149 (2014) 151–158.
[20] J.K. Im, I.H. Cho, S.K. Kim, K.D. Zoh, Optimization of carbamazepine removal in O_3/UV/H_2O_2 system using a response surface methodology with central composite design, Desalination 285 (2012) 306–314.

[21] C.T. Jafvert, R.L. Valentine, Reaction scheme for the chlorination of ammoniacal water, Environ. Sci. Technol. 26 (1992) 577–586.
[22] H. Gallard, U.V. von Gunten, Chlorination of natural organic matter: Kinetics of chlorination and of THM formation, Water Res. 36 (2002) 65–74.
[23] J.R Bolton, D.W. Smith, J.R. Bolton, Photolysis of aqueous free chlorine species (HOCl and OCl–) with 254 nm ultraviolet light, J. Environ. Eng. Sci. 6 (2007) 277–284.
[24] D. Wang, J.R. Bolton, R. Hofmann, Medium pressure UV combined with chlorine advanced oxidation for trichloroethylene destruction in a model water, Water Res. 46 (2012) 4677–4686.